Clinical Neurophysiology Practice 5 (2020) 16–22

Contents lists available at ScienceDirect

Clinical Neurophysiology Practice

journal homepage: www.elsevier.com/locate/cnp

Research paper

Visual analysis of high density EEG: As good as electrical source imaging?

Gianpaolo Toscano [a,b,c,*], Margherita Carboni [a,d], Maria Rubega [d], Laurent Spinelli [a], Francesca Pittau [a], Andrea Bartoli [e], Shahan Momjian [e], Raffaele Manni [b], Michele Terzaghi [b,c], Serge Vulliemoz [a], Margitta Seeck [a]

[a] EEG and Epilepsy Unit, University Hospital of Geneva, Geneva, Switzerland
[b] Unit of Sleep Medicine and Epilepsy, IRCCS Mondino Foundation, Pavia, Italy
[c] Department of Brain and Behavioural Sciences, University of Pavia, Italy
[d] Functional Brain Mapping Lab, Department of Fundamental Neurosciences, University of Geneva, Geneva, Switzerland
[e] Department of Neurosurgery, University Hospital of Geneva, Geneva, Switzerland

ARTICLE INFO

Article history:
Received 3 August 2019
Received in revised form 19 September 2019
Accepted 29 September 2019
Available online 30 November 2019

Keywords:
High density EEG
Epilepsy surgery
Source analysis
Focus localization
MRI
Electric source imaging

ABSTRACT

Objective: In this study, we sought to determine whether visual analysis of high density EEG (HD-EEG) would provide similar localizing information comparable to electrical source imaging (ESI).
Methods: HD-EEG (256 electrodes) recordings from 20 patients suffering from unifocal, drug-resistant epilepsy (13 women, mean age 29.1 ± 2.62 years, 11 with temporal lobe epilepsy) were examined. In the visual analysis condition, we identified the 5 contacts with maximal spike amplitude and determined their localization with respect to the underlying cortex. ESI was computed using the LAURA algorithm of the averaged spikes in the patient's individual MRI. We considered the localization "correct" if all 5 contacts were concordant with the resection volume underneath or if ESI was located within the resection as determined by the postoperative MRI.
Results: Twelve patients were postoperatively seizure-free (Engel Class IA), while the remaining eight were in class IB to IV. Visual analysis and ESI showed sensitivity of 58% and 75%, specificity of 75% and 87%, and accuracy of 65% and 80%, respectively. In 70% of cases, visual analysis and ESI provided concordant results.
Conclusions: Localization of the electrodes with maximal spike amplitude provides very good estimation of the localization of the underlying source. However, ESI has a higher accuracy and adds 3D information; therefore, it should remain the tool of choice for presurgical evaluation.
Significance: The present study proposes the possibility to analyze HD-EEG visually, in tandem with ESI or alone, if ESI is not accessible.

1. Introduction

For patients who are not seizure-free despite adequate therapy with antiepileptic drugs (AEDs), surgery is an important option that could result in seizure resolution or significant improvement (Engel, 1996). In patients with refractory focal epilepsy, the ideal surgery should disconnect or remove the epileptogenic zone (EZ), i.e., the brain area whose surgical removal is required and is sufficient to render the patient seizure-free (Lüders et al., 2006). The accurate delineation of the EZ is important, and this area is estimated by localizing the Seizure Onset Zone (SOZ, which is the area of the cortex indispensable for the generation of epileptic seizures) and the Irritative Zone (IZ, which is the area of cortical tissue that generates Interictal Epileptiform Discharges, IEDs) (Rosenow and Lüders, 2001). Other sources of information include magnetic resonance imaging (MRI), single-photon emission computed tomography (SPECT), positron emission tomography (PET), magnetoencephalography (MEG), electroencephalography-correlated functional magnetic resonance imaging (fMRI-EEG), and invasive electroencephalography (iEEG). EEG plays a central role in the diagnosis and management of patients with seizure disorders and contributes to the multiaxial diagnosis of epilepsy (Smith, 2005). Interictal spikes and/or sharp waves are considered as an excellent estimate of the SOZ in the majority of patients (Mégevand et al., 2014). They are characterized by a higher signal-to-noise ratio (SNR) and are less contaminated by muscular

* Corresponding author at: Unit of Sleep Medicine and Epilepsy, IRCCS Mondino Foundation, Via Mondino 2, 27100 Pavia, Italy.
E-mail address: gianpaolo.toscano@mondino.it (G. Toscano).

https://doi.org/10.1016/j.cnp.2019.09.002
2467-981X/

artifacts than ictal events; in addition, they are more likely to be captured during a recording session of limited duration (Nemtsas et al., 2017). Electrical source imaging (ESI) using interictal discharges has been proven to be highly localizing, and ESI based on HD-EEG is now an established tool to localize the SOZ (Mégevand et al., 2014; Lantz et al., 2003a,2003b; Yamazaki et al., 2013; Michel et al., 2004; Brodbeck et al., 2009; Brodbeck et al., 2010). However, it requires a complicated workflow, expert staff members, and specific softwares such as Cartool (https://sites.google.com/site/cartoolcommunity/files) or GeoSource (https://www.egi.com/research-division/electrical-source-imaging/geosource). While the yield of ESI for focus localization has been well studied, no data are available about HD-EEG localization by visual analysis. Thus, we were interested in investigating whether visual analysis of HD-EEG has a comparable efficacy as ESI to localize the epileptogenic focus.

2. Methods

2.1. Patients

Patients were selected from those admitted for presurgical evaluation to the EEG & Epilepsy Unit, Department of Clinical Neurosciences, University Hospital of Geneva, Switzerland. The inclusion criteria were as follows: 1) patients suffering from focal, refractory epilepsy; 2) patients who underwent HD-EEG (256 channels) long-term (>4h) recording; 3) patients having at least 10 detectable IEDs on scalp EEG; 4) patients who underwent brain surgery for focal epilepsy; and 5) patients for whom both preoperative and postoperative MRI data were available. Exclusion criteria were as follows: 1) patients with multifocal epilepsy; 2) patients who already underwent a brain surgery for epilepsy in the same area or another surgical brain intervention that could influence the EEG (breach rhythm) and/or ESI localization in a significant way.

In our database, 22 surgical patients were identified. Two were excluded because they did not show enough IEDs during the recording. The remaining 20 patients (65% women, 29.1 ± 2.62 years, 11 with temporal lobe epilepsy) fully met the inclusion criteria. During the presurgical evaluation, all the patients underwent neurological examination, low- and high-density video-EEG monitoring, high resolution 3 T MRI with an epilepsy-specific protocol, PET, and if possible, SPECT and neuropsychological evaluation. For logistical reasons, HD-EEG was recorded at the end of the hospitalization, i.e., after clinical 31–38 electrode routine recordings of 4–14 days. Table 1 summarizes the clinical data of the 20 patients.

2.2. HD-EEG recordings

All patients underwent HD-EEG long-term monitoring (LTM) using a 256-electrode scalp EEG system. Duration of recordings was between 4 and 20 h. The HD-EEG was recorded with the Geodesic Sensor Net with interconnected electrodes (Electrical Geodesic, Inc., Eugene, OR, U.S.A.), placed to the scalp according to the international 10/10 system, using a conductive paste. The tension structure of the net ensured that all electrodes were evenly distributed over the scalp, using natural fiduciaries such as inion and nasion, at the same location across patients. Electrode-skin impedances were maintained at <15 kΩ. The recordings were sampled at 1 kHz, referenced to Cz, and passed through a 0.5- to 70-Hz band-pass filter.

2.3. HD-EEG visual examination and IED selection

To detect and select the IEDs, an epileptologist (G.T.), blinded to the patient's name and clinical information, analyzed the recorded HD-EEG data. The visual analysis started using a shortened bipolar reading montage, i.e., extended double-banana, with the inferior electrode chain covering the basal fronto-orbital, temporal, and temporo-occipital cortex. Criteria for IED selection were as follows: IEDs homogeneous for morphology and topography in each patient, representative for the patient's EEG as determined by the review of the remaining long-term EEG. For each HD-EEG recording, all IEDs were marked, but only the 10 IEDs (spikes or sharp waves) with highest SNR were selected. The IEDs were marked at the exact time point of maximal negativity on the electrode trace with the highest amplitude. After the 10 IEDs were selected for each patient, the HD-EEG was checked carefully for their scalp distribution by using an average reference montage (AVG) in which the 5 contacts with maximal amplitude were selected for each IED.

2.4. Comparison between visual EEG results and post-op imaging

For each patient, we identified the electrodes supposed to be involved in the EZ, as described above. Thus, a total of 50 electrodes, resulting from 5 contacts × 10 IEDs, were obtained for each patient. The 5 most frequent electrodes out of the 50 electrodes were considered representative of the patient's IZ. For each patient, the postoperative MRI was co-registered with the EEG-electrodes coordinates in the same space. A 3D reconstruction of the resected zone, and its center, called centroid, were obtained, and the Euclidian distance between the centroid of the 3D reconstruction and each of the 256 electrodes was computed using MATLAB® R2018b (https://www.mathworks.com/products/matlab.html). Thirteen out of 256 contacts (5%) nearest to the centroid were considered as Reference-Electrodes (RE). If 5 out of 5 electrodes (100%) marked by visual inspection were concordant with the RE, the localization was considered fully concordant. Fig. 1 shows an example of visual localization of IED and comparison with post-op imaging.

2.5. Electrical source imaging (ESI)

The HD-EEG data were filtered (high-pass filter: 0.5 Hz; low-pass filter: 70 Hz; notch: 50 Hz) using a 3rd order Butterworth filter by avoiding phase distortion; bad channels were excluded and interpolated. The average of the 10 pre-processed spikes was the input for ESI. Both EEG preprocessing and the inverse solution were performed by freely available software Cartool (https://sites.google.com/site/cartoolcommunity/files) (Brunet et al., 2011).

The grey matter was extracted from the individual preoperative T1 MRI to constrain circa 5000 solution points into the gray matter on a regular grid of 6 mm resolution. The scalp electrodes were co-registered with the individual T1 preoperative MRI using a template cap to correctly place Fpz, Cz, Oz, and pre-auricular points according to the international 10/10 system. Eventually, the template cap electrodes were projected onto the head surface. The locally spherical model with anatomical constraints (LSMAC) head model, as performant as boundary element model (BEM) and finite element model (FEM) for ESI of interictal spikes, was used (Birot et al., 2014).

For the inverse solution, the linear inverse method called LAURA (Grave de Peralta Menendez et al., 2001; Grave de Peralta Menendez et al., 2004), implemented in Cartool, was used. Because LAURA cannot determine the spatial extent of cortical activation, only the solution point with the maximal magnitude (ESI-max) and the circle with a radius of 6 mm around ESI max point, automatically generated by Cartool, were considered as ESI localization. For further details on the ESI pipeline, we refer the reader to earlier descriptions and to the specific methodological literature (National Research Council, 1996). Previous studies reported the importance of considering the average of the IED at the 50% of the rising phase

Table 1
Clinical data and interictal pattern. Legend: M male, F female, R right, L left, F frontal, T temporal, P parietal, O occipital.

PATIENT	Sex	Age of epilepsy onset (y)	Age at surgery	Outcome (Engel Class)	Surgical area	Lesion type	Scalp monitoring – EEG Visual Analysis	Scalp HD – EEG Visual Analysis	ESI – 50%	ESI – peak	Concordance/ Discordance between Scalp HD and ESI Results
PAT 1	F	18	21	I A	R orbito-frontal resection	–	Right FT	2/5	Inside	Inside	Discordant
PAT 2	M	9	29	I A	R lateral temporal resection	Cavernous hemangioma	Right FT	2/5	Outside (23.31 mm)	Outside (23.31 mm)	Concordant
PAT3	F	3	44	I A	R amygdalo-hippocampectomy and temporal polectomy	–	Right FT	5/5	Inside	Inside	Concordant
PAT 4	F	7	31	II A	L frontal resection	Cortical dysplasia	Left F	3/5	Outside (19.99 mm)	Outside (30.75 mm)	Concordant
PAT 5	F	9	12	I A	L fronto-parietal interhemispheric resection	Cortical dysplasia	Left FC	5/5	Outside (31.2 mm)	Outside (31.2 mm)	Discordant
PAT6	F	6	10	I A	L amygdalo-hippocampectomy and temporal polectomy	Cortical dysplasia	Left T	5/5	Inside	Inside	Concordant
PAT 7	M	20	37	I A	R amygdalo-hippocampectomy	Hippocampal sclerosis	Right FT	3/5	Inside	Inside	Discordant
PAT 8	F	11	30	I A	R temporal Polectomy	Cortical dysplasia	Right FT	5/5	Inside	Inside	Concordant
PAT 9	M	10	30	I A	R amygdalo-hippocampectomy and temporal polectomy	Cortical dysplasia	Right T	4/5	Inside	Inside	Discordant
PAT 10	M	22	28	I A	L temporal Anterior resection	Hippocampal sclerosis	Left T	5/5	Inside	Inside	Concordant
PAT 11	F	14	27	I D	L parieto-opercular resection	Cortical dysplasia	Left T	1/5	Outside (17.5 mm)	Outside (17.5 mm)	Concordant
PAT 12	F	28	37	I D	L temporal polectomy	Ganglioglioma	Left FT	5/5	Inside	Inside	Concordant
PAT 13	M	25	32	I A	R amygdalo-hippocampectomy and temporal polectomy	Hippocampal sclerosis	Right FT	5/5	Inside	Inside	Concordant
PAT 14	F	11	19	I A	L temporal posterior resection	Cortical dysplasia	Left TP	2/5	Outside (15.2 mm)	Outside (15.2 mm)	Concordant
PAT 15	F	9 months	13	III A	L frontal resection	Cortical dysplasia and heterotopy	Left FP	0/5	Outside (40.2 mm)	Outside (59.3 mm)	Concordant
PAT 16	F	12	21	III A	L premotor cortectomy	Perinatal Lesion	Left F	3/5	Outside (36.1 mm)	Outside (36.1 mm)	Concordant
PAT 17	F	24	53	II C	R temporal anterior resection	–	Right T	5/5	Outside (11.2 mm)	Outside (9 mm)	Discordant
PAT 18	M	34	44	III A	L parieto-Occipital resection	Tumor	Left TP	0/5	Outside (75.23 mm)	Outside (22.49 mm)	Concordant
PAT 19	M	17	44	I A	L amygdalo-hippocampectomy and Temporal polectomy	Hippocampal sclerosis	Left T	5/5	Inside	Inside	Concordant
PAT 20	F	9	20	IV B	R frontal	Cortical dysplasia	Bilateral FT	2/5	Inside	Outside (14.1 mm)	Discordant

(Lantz et al., 2003a,2003b), which was also used for the present study.

In a second analysis, for each patient, both the ESI localizations, at 50% of the spike slope and spike peak, were calculated, and the distance between the two different localizations was compared with the post-surgical outcome.

Fig. 2 shows examples of concordant and discordant ESI localizations at spike peak and at 50% of the spike slope.

2.6. Statistical analysis

For both the visual inspection HD-EEG method and the ESI, we calculated the number of true positive (TP), false positive (FP), true negative (TN), and false negative (FN) based on the post-surgery outcome (Table 2). Only patients in the Engel class IA were considered as seizure-free, and the remainder as nonseizure-free.

We considered as TP the number of seizure-free patients in whom all the 5 electrodes with IEDs of maximal amplitude were among the RE; as FP, the non-seizure free patients in whom all IED electrodes were among the RE; as TN, the non-seizure free patients in whom less than 5 electrodes were part of RE; and as FN, the seizure-free patients in whom less than 5 electrodes were part of RE.

For the ESI, we considered as TP, the seizure-free patients in whom the maximum of the ESI was localized into the resected area; as FP, the nonseizure-free patients in whom the maximum of the ESI was localized into the resected area; as TN, the nonseizure-free patients in whom the maximum of the ESI was

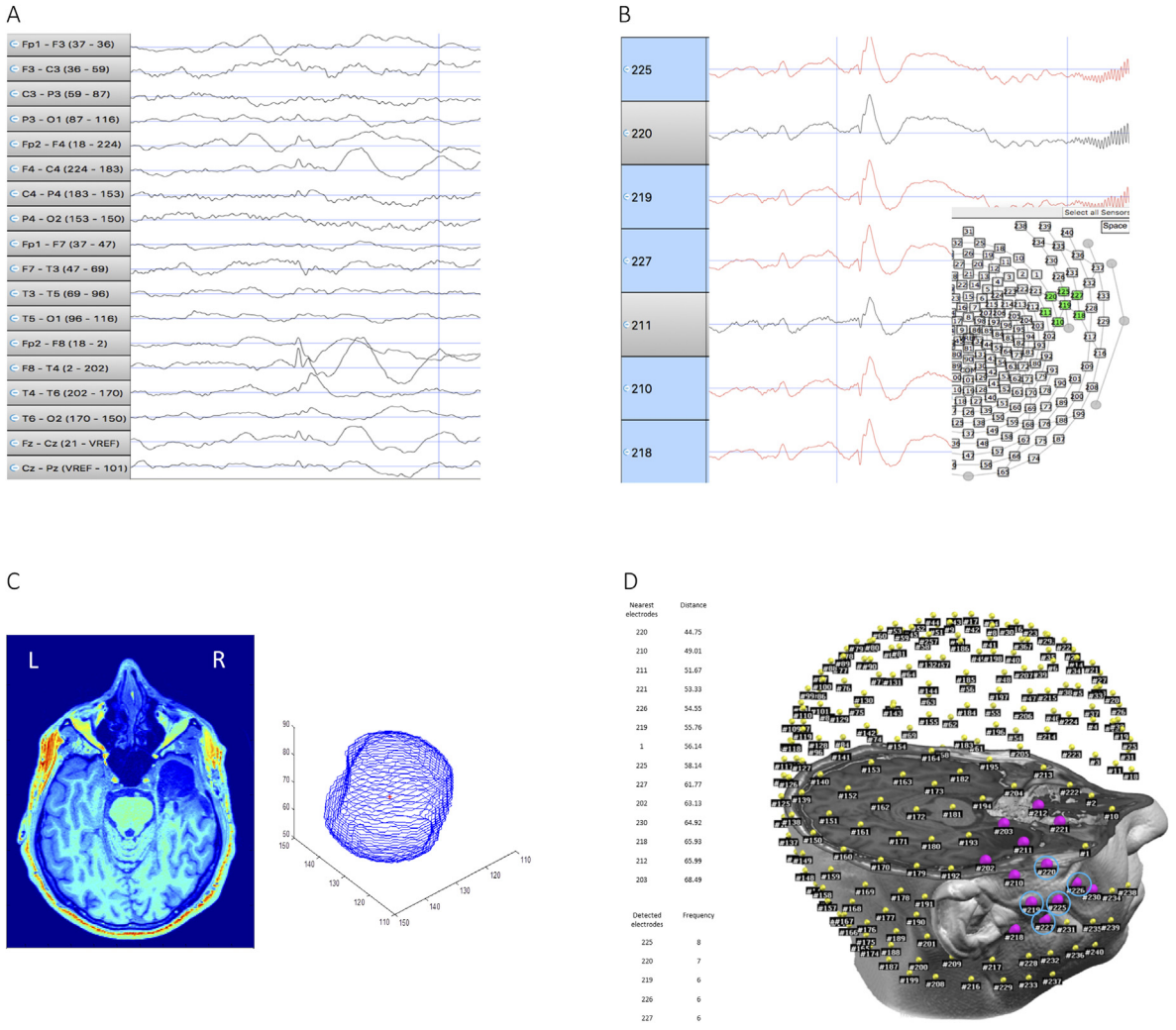

Fig. 1. Example of method for spike selection and comparison between visual EEG results and Reference-Electrodes (RE) (PAT 13 in Table 1). A) Identification of the IED on standard montage. B) interictal discharge displayed using AVG referential montage; the 5 electrodes in which the signal is wider are selected (red-marked). C) *Left:* postoperative MRI showing right temporal resection. *Right:* 3D reconstruction of the removed area; the centroid of the resected zone is marked in red. D) *Left:* Top, table showing the nearest 13 electrodes (5% of 256) to the resected zone (RE); Bottom, table showing the 5 electrodes marked by visual analysis. *Right:* electrodes coregistered on the head of the patient; the RE are marked in purple; the 5 electrodes identified by visual analysis are rounded by a blue circle. In this case, all the 5 electrodes detected by the epileptologist were inside the RE; hence, for this patient, the visual analysis localization has been considered fully correct.

localized outside the resected area; and as FN, the seizure-free patients in whom the maximum of the ESI was localized outside the resected area.

For both methods, we calculated accuracy as the ratio between the sum of TP and TN and the number of subjects; sensitivity as the ratio between TP and the sum of TP and FN; and specificity as the ratio between the TN and the sum of TN and FP (Baratloo et al., 2015).

A nonparametric *t*-test (Wilcoxon rank sum test) ($p < 0.05$) was applied to compare the number of electrodes found in patients with ESI pointing inside the resected area versus the number of electrodes found in patients with ESI outside the resected area.

To compare the performance of the two analyzed techniques - visual analysis and ESI - in patients with different recovery rates after surgery, we applied the same nonparametric *t*-test (Wilcoxon rank sum test) ($p < 0.05$). The patients were divided in three groups: seizure-free (Engel IA), almost seizure-free (IB-IID), and nonseizure-free (III-IV). A regression coefficient based on the outcome was calculated for both the visual inspection method and ESI.

3. Results

Table 2 shows the results of the interictal localization in standard EEG, HD-EEG, ESI at 50% of the spike slope, and at spike peak. In Fig. 3, the values of sensitivity, specificity and accuracy for both the analyzed techniques are shown. For visual analysis, sensitivity, specificity, and accuracy were 58%, 75%, and 65%, respectively. ESI, providing direct 3D images of the underlying source, had a sensitivity of 75%, a specificity of 87%, and an accuracy of 80%. In one case (patient No 4, left fronto-parietal dysplasia), ESI indicated wrong localization, but visual inspection localized correctly the IZ. The two methods (visual analysis and ESI) provided concordant results in 70% of patients ($n = 14$); of the discordant cases ($n = 6$), 4 were correctly localized only by ESI and 2 by visual analysis.

For patients in which ESI located the maximum of electrical activity inside the resected area, a higher number of electrodes was found among RE at the visual analysis than in the ESI-outside patients ($p = 0.01$).

Patients who were completely seizure-free (Engel IA, $N = 12$) showed significantly more electrodes recognized by the epileptol-

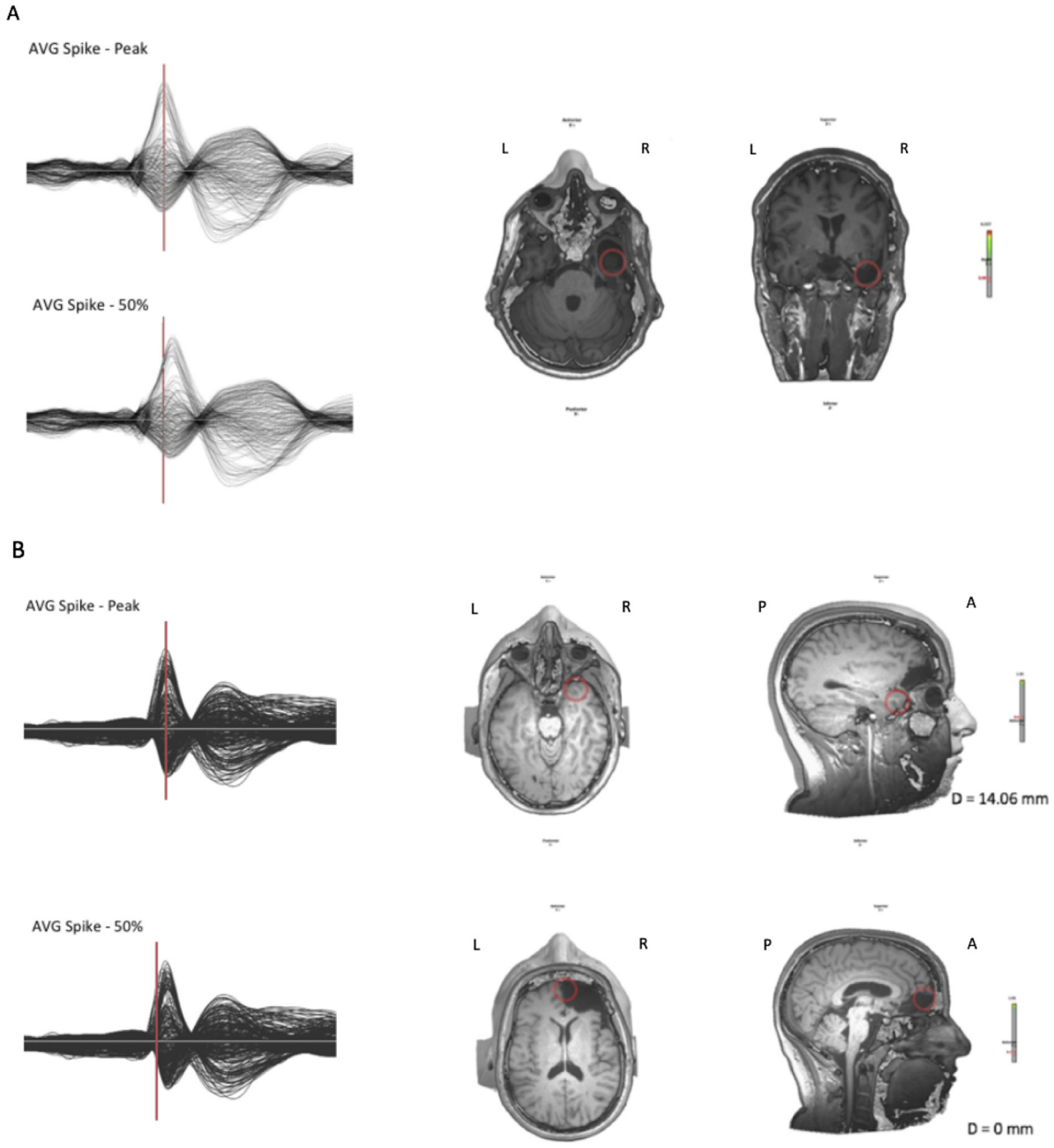

Fig. 2. Examples of concordant (A) and discordant (B) ESI localizations at spike peak and 50% of spike slope. Legend: A anterior, P posterior, R right, L left. A Same patient shown in Fig. 1, good outcome - Engel IA (PAT 13 in Table 1). *Left:* Top, average spike with cursor pointed at the peak of the spike; bottom, cursor pointed at 50% of the rising phase. *Right:* Transversal and frontal section of MRI showing ESI. In this case, ESI obtained at the 50% of the spike slope and at spike peak both pointed inside the resected area. B Poor outcome patient - Engel IV B (PAT 20 in Table 1). *Left:* Top, average spike with cursor pointed at the peak of the spike; bottom, cursor pointed at 50% of the rising phase. *Right:* Transversal and frontal section of MRI showing ESI. In this case, ESI obtained at the 50% of the spike slope and at spike peak localize the source in two different brain areas.

Table 2
The number of patients classified as TP (true positive), FP (false positive), TN (true negative), and FN (false negative) for the two methods.

# of Patients	TP	FP	TN	FN
Visual analysis	7/20	2/20	6/20	5/20
ESI	9/20	1/20	7/20	3/20

ogist as indicative of the IZ than those with poor outcome (Engel III and IV, N = 4; p = 0.02).

Comparing ESI at both the 50% of the spike slope and at the peak of the spike, a strong trend of larger distances was observed between both ESI solutions in patients with less good outcome. The distance between the two localizations was significantly smaller between the seizure-free or almost seizure-free patients (from IA to IID, N = 16) and those with poor outcome (III-IV) (p = 0.05, N = 4) (Fig. 4).

4. Discussion

ESI is a validated noninvasive method to localize the epileptogenic focus using patient's individual MRI (Brodbeck et al., 2011); however, it requires advanced computer skills and use of sophisti-

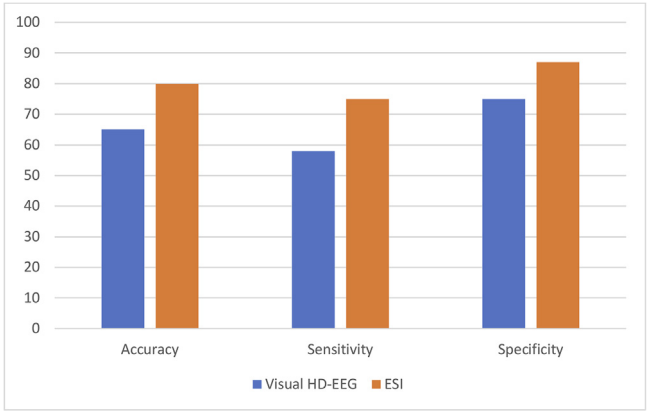

Fig. 3. Comparison between Visual HD-EEG analysis (blue column) and ESI (orange column) in terms of accuracy, sensitivity, and specificity.

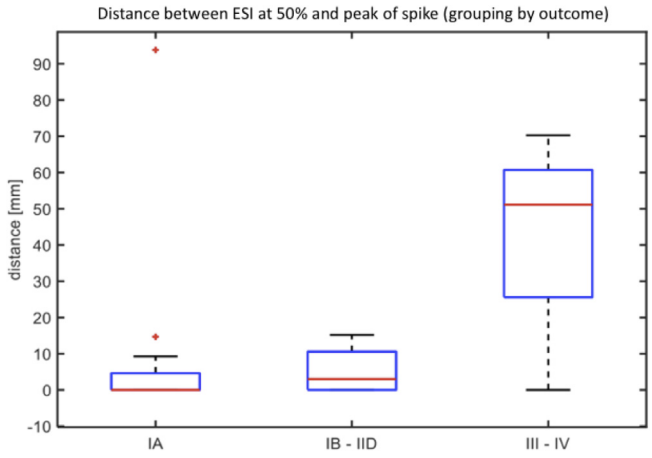

Fig. 4. Boxplot Graph – Comparison between ESI at 50% and ESI at peak. X axis: outcomes of the patients (Engel Class) - Y axis: distance between ESI (50% of the rising phase) and ESI (peak). The distance between the two ESI localizations increases with the worsening of the outcomes of the patients (for IA versus III-IV, p = NS; for IA to IID versus III-IV, p = 0.05).

cated algorithms. Most commercial programs require a learning period of several weeks to months to develop proficiency in proper data managing. Additionally, procedures such as co-registration of patient's MRI are time-consuming and difficult to fit into a busy clinical schedule. In the present study, we wanted to determine whether visual analysis of HD-EEG would localize the focus reasonably well.

We demonstrated that visual analysis, i.e., the determination of electrodes with maximal amplitude, provides a good first estimate of the approximate focus localization, albeit not as good as ESI. Such an analysis technique can nevertheless still be useful, in that it could suggest the need for patient's MRI or PET of the suspicious region and potentially identify small lesions that were missed on the first reading. Visual analysis provided an accuracy of 65% through applying strict rules by considering "correct" 5/5 electrodes overlaying the resected zone. In one patient, this kind of analysis provided a better result than ESI, which suggests that it could be used in tandem with ESI.

An intrinsic limitation of our purposed method is that scalp EEG could lead to false localizations, while voltage maps and thus ESI, can better estimate cortical generators. Indeed, ESI provides higher sensitivity and specificity values (75% and 87%, respectively), with respect to our reference standard of complete seizure control, and were similar to previous studies (Brodbeck et al., 2010; Habib et al., 2016). While ESI is a more work-intensive technique, it provides 3D solutions in the patient's MRI and its localizing value is excellent than those of other established imaging techniques (Lascano et al., 2016). ESI should be therefore considered as the analysis of choice, especially for patients in whom MRI does not show evidence of an underlying lesion or have multifocal lesions (Brodbeck et al., 2010).

Our analysis started with reading the EEG using low-density bipolar EEG montages (extended double-banana) to identify the IEDs, and we then switched to the common average montage for more precise evaluation of the interictal zone. This approach corresponds to clinical practice when reviewing long-term EEG, but is suboptimal, because it may miss foci, if they are not reflected in the electrodes of the bipolar montage. This may contribute to the lower sensitivity and accuracy of visual analysis. Software allowing the automatic identification of IEDs in 256 channel EEGs would be of utmost help, but thus far, most algorithms have been inferior to the naked eye, given the variable morphology of IEDs and the presence of frequent spike mimics like certain sleep pattern and movement artefacts. Moreover, extratemporal spikes are much less well captured by automatic spike detection programs, but promising algorithms have been developed in recent 10–15 years (van Mierlo et al., 2017). A novel method of reconstructing MEG signals in the source space (Beniczky et al., 2016) could be also useful for HD-EEG, facilitating the visual review of the EEG significantly.

A limitation of our study is its retrospective nature and the small number of patients. However, our results allow the proof of concept that HD-EEG of 256 channels can also be analysed "traditionally" and the increased number of electrodes allow very good visual localization.

Data from previous ESI studies showed that intraspike propagation occurs. Therefore, it was proposed to use the 50% rising phase for ESI localization, which was correct in all the explored cases (Lantz et al., 2003a,2003b). In our study, we were interested in exploring the relationship between the two phases of the spike and the postoperative outcome. Comparing ESI obtained from the peak of the IED and the 50% of its rising phase, we noted a strong trend of discordancy in patients who were not seizure-free. On the contrary, results tended to match for good-outcome patients. It is possible that good outcome patients show "more stable" spikes, which remain within a defined volume during the entire duration of the interictal discharge; good outcome patients could eventually have more limited IZ and SOZ, which would be more likely be included in the resection volume. On the other hand, patients with suboptimal surgical resuts would show a more variable sequence of remote brain regions recruitment. If confirmed in a larger cohort, the computation of ESI at 50% of the rising phase and at the peak of the spike separately could be used as a biomarker to identify patients who need broader surgical resections or intracranial monitoring in order to increase the likelihood of postoperative seizure control.

5. Conclusion

Visual analysis of HD-EEG is an easy and valid technique to estimate the localization of the interictal focus, which most often corresponds to the ictal onset zone. It can be performed without access to source localization algorithms or the knowledge to create the technical pipeline, necessary for ESI. However, ESI provides better accuracy and should remain the gold standard for scalp source localization in presurgical evaluation.

Ethical Publication Statement

We confirm that we have read the Journal's position on issues involved in ethical publication and affirm that this report is consistent with those guidelines.

Declaration of Competing Interest

The authors declare that they have no known competing financial interests or personal relationships that could have appeared to influence the work reported in this paper.

References

Baratloo, A., Hosseini, M., Negida, A., El Ashal, G., 2015. Part I: Simple definition and Calculation of Accuracy, Sensitivity and Specificity. Emerg (Tehran) 3, 48–49.

Beniczky, S., Duez, L., Scherg, M., Orm Hansen, P., Tankisi, H., Sidenius, P., et al., 2016. Visualizing spikes in source-space: Rapid and efficient evaluation of magnetoencephalography. Clin. Neurophysiol. 127 (2), 1067–1072.

Birot, G., Spinelli, L., Vulliémoz, S., Mégevand, P., Brunet, D., Seeck, M., et al., 2014. Head model and electrical source imaging: a study of 38 epileptic patients. Neuroimage Clin. 5, 77–83.

Brodbeck, V., Lascano, A.M., Spinelli, L., Seeck, M., Michel, C.M., 2009. Accuracy of EEG source imaging of epileptic spikes in patients with large brain lesions. Clin. Neurophysiol. 120 (4), 679–685.

Brodbeck, V., Spinelli, L., Lascano, A.M., Pollo, C., Schaller, K., Vargas, M.I., et al., 2010. Electrical source imaging for presurgical focus localization in epilepsy patients with normal MRI. Epilepsia 51 (4), 583–591.

Brodbeck, V., Spinelli, L., Lascano, A.M., Wissmeier, M., Vargas, M.I., Vulliémoz, S., et al., 2011. Electroencephalographic source imaging: a prospective study of 152 operated epileptic patients. Brain 134, 2887–2897.

Brunet, D., Murray, M.M., Michel, C.M., 2011. Spatiotemporal analysis of multichannel EEG: CARTOOL. Comput. Intell. Neurosci. 2011, 813870.

Engel, J., 1996. Surgery for seizures. N. Engl. J. Med. 334 (10), 647–652.

Grave de Peralta Menendez, R., Gonzalez Andino, S., Lantz, G., Michel, C.M., Landis, T., 2001. Noninvasive localization of electromagnetic epileptic activity. I. Method descriptions and simulations. Brain Topogr. 14 (2), 131–137.

Grave de Peralta Menendez, R., Murray, M., Michel, C.M., Martuzzi, R., 2004. Gonzalez Andino SL. Electrical neuroimaging based on biophysical constraints. Neuroimage 21 (2), 527–539.

Habib, M.A., Ibrahim, F., Mohktar, M.S., Kamaruzzaman, S.B., Rahmat, K., Lim, K.S., 2016. Ictal EEG source imaging for presurgical evaluation of refractory focal epilepsy. World Neurosurg. 88, 576–585.

Lantz, G., Spinelli, L., Seeck, M., de Peralta Menendez, R.G., Sottas, C.C., Michel, C.M., 2003b. Propagation of interictal epileptiform activity can lead to erroneous source localizations: a 128-channel EEG mapping study. J. Clin. Neurophysiol. 20 (5), 311–319.

Lantz, G., Grave del Peralta, R., Spinelli, L., Seeck, M., Michel, C.M., 2003a. Epileptic source localization with high density EEG: how many electrodes are needed? Clin. Neurophysiol. 114 (1), 63–69.

Lascano, A.M., Perneger, T., Vulliémoz, S., Spinelli, L., Garibotto, V., Korff, C.M., 2016. Yield of MRI, high-density electric source imaging (HD-ESI), SPECT and PET in epilepsy surgery candidates. Clin. Neurophysiol. 127 (1), 150–155.

Lüders, H.O., Najm, I., Nair, D., Widdess-Walsh, P., Bingman, W., 2006. The epileptogenic zone: General principles. Epileptic Disord (Suppl 2), S1–S9.

Mégevand, P., Spinelli, L., Genetti, M., Brodbeck, V., Momjan, S., Shaller, K., et al., 2014. Electric source imaging of interictal activity accurately localises the seizure onset zone. J. Neurol. Neurosurg. Psychiatry 85 (1), 38–43.

Michel, C.M., Murray, M.M., Lantz, G., Gonzalez, S., Spinelli, L., Grave de Peralta, R., 2004. EEG source imaging. Clin. Neurophysiol. 115 (10), 2195–2222.

National Research Council, 1996. Mathematics and Physics of Emerging Biomedical Imaging. The National Academies Press, Washington, DC.

Nemtsas, P., Boirot, G., Pittau, F., Michel, C.M., Schaller, K., Vulliémoz, S., 2017. Soure localization of ictal epileptic activity based on high-density scalp EEG data. Epilepsia 58, 1027–1036.

Rosenow, F., Lüders, H.O., 2001. Presurgical evaluation of epilepsy. Brain 124, 1683–1700.

Smith, S.J., 2005. EEG in the diagnosis, classification and management of patients with epilepsy. J. Neurol. Neurosurg. Psychiatry 76 (Suppl 2). ii2–ii7.

van Mierlo, P., Strobbe, G., Keereman, V., Birot, G., Gadeyne, S., Gschwind, M., et al., 2017. Automated long-term EEG analysis to localize the epileptogenic zone. Epilepsia Open 2 (3), 322–333.

Yamazaki, M., Tucker, D.M., Terrill, M., Fujimoto, A., Yamamoto, T., 2013. Dense array EEG source estimation in neocortical epilepsy. Front. Neurol. 4, 42.